Supporting Information:

S.1.1. Core Code for Gaussian Process Regression (GPR)

```
from sklearn.preprocessing import StandardScaler; from sklearn.gaussian_process import GaussianProcessRegressor; from sklearn.gaussian_process.kernels import RBF, WhiteKernel; from sklearn.metrics import mean_absolute_error, mean_squared_error, r2_score; import numpy as np
class GaussianProcessModel:
    def __init__(s): s.sc=StandardScaler(); s.m=GaussianProcessRegressor(RBF(1.0,(1e-2,1e3))+WhiteKernel(1,(1e-5,1e3)),alpha=1e-5,n_restarts_optimizer=15,random_state=42)
    def train(s,X,y): s.m.fit(s.sc.fit_transform(X),y)
def evaluate(s,X,y): p,_=s.m.predict(s.sc.transform(X),return_std=True); return {"MAE":mean_absolute_error(y,p),"MSE":mean_squared_error(y,p),"RMSE":np.sqrt(mean_squared_error(y,p)),"R2":r2_score(y,p)}
```

S.1.2. Core Code for Data Processing

```
import pandas as pd, numpy as np; from sklearn.impute import SimpleImputer; from sklearn.model_selection import train_test_split
class DataProcessor:
    def __init__(s,f): s.df=pd.read_excel(f); s.df.columns=s.df.columns.str.replace('（','(').str.replace('）',')'); s.df.rename({'Phosphorus-containing wastewater with different concentrations':'Experiment_Type','Al(mg/L)':'Al','Fe(mg/L)':'Fe','Ca(mg/L)':'Ca','Al_ Phosphorus recovery (%)':'Al_recovery','Fe_ Phosphorus recovery (%)':'Fe_recovery','Ca_ Phosphorus recovery (%)':'Ca_recovery','Phosphorus recovery equilibrium time(min)':'Equilibrium_time'},axis=1,inplace=True)
    def clean(s): s.df=s.df.applymap(lambda x: eval(x) if isinstance(x,str) and x.startswith('=') else x); s.df['Fe']=np.where(s.df.Experiment_Type.eq(1),s.df.Fe,0); s.df['Al']=np.where(s.df.Experiment_Type.eq(2),s.df.Al,0); s.df['Ca']=np.where(s.df.Experiment_Type.eq(3),s.df.Ca,0); s.df['Fe_recovery']=np.where(s.df.Experiment_Type.eq(1),s.df.Fe_recovery,np.nan); s.df['Al_recovery']=np.where(s.df.Experiment_Type.eq(2),s.df.Al_recovery,np.nan); s.df['Ca_recovery']=np.where(s.df.Experiment_Type.eq(3),s.df.Ca_recovery,np.nan); cols=['Time(min)','Temperature(℃)','Mixing speed(rpm)','pH','inorganic phosphate(mg/L)']; s.df[cols]=SimpleImputer(strategy='median').fit_transform(s.df[cols]); s.df['Equilibrium_time']=s.df['Equilibrium_time'].fillna(s.df['Time(min)'])
    def split(s,target,test_size=0.2,random_state=42): m={'Fe_recovery':1,'Al_recovery':2,'Ca_recovery':3}; d=s.df if target=='Equilibrium_time' else s.df[(s.df.Experiment_Type==m[target])&s.df[target].notna()]; base=['Time(min)','Temperature(℃)','Mixing speed(rpm)','pH','inorganic phosphate(mg/L)']; add=(['Fe'] if target.startswith('Fe_') else ['Al'] if target.startswith('Al_') else ['Ca'] if target.startswith('Ca_') else ['Al','Fe','Ca']); X,y=d[base+add],d[target]; return train_test_split(X,y,test_size=test_size,random_state=random_state)
```

S.2.Analysis of Anomalous Results

In the aluminum-based experimental group, the anomalous phenomenon of phosphorus recovery rates exceeding 200% can be attributed to several interrelated factors.

Firstly, measurement inaccuracies in influent and effluent concentrations play a critical role, particularly when the influent total phosphorus (TP) approaches the detection limit, where even minor deviations (e.g., ±0.02 mg/L) can be disproportionately amplified in recovery calculations, an issue compounded by transient phosphorus release‐reabsorption dynamics during sampling that may artificially inflate results [41].

Secondly, inconsistencies in unit conversions—such as between total phosphorus (P) and orthophosphate (PO_4^{3-}-P) expressed as mg/L or μmol/L—along with inappropriate baseline settings, can introduce systematic biases capable of producing such excessive values [42].

Furthermore, short-term kinetic effects inherent to aluminum coagulation, wherein phosphorus is temporarily released and subsequently re-captured, may lead to underestimation of effluent TP if sampling coincides with this transient window, thereby elevating apparent recovery [43].

Finally, reliance on empirical or equilibrium models for data interpretation presents risks when experimental conditions extend beyond the model's calibration range, as high aluminum doses may induce complex side reactions or secondary dissolution phenomena not fully accounted for in simulations, thus yielding theoretically implausible recovery rates [44].

S.3.Analysis of Anomalous Results

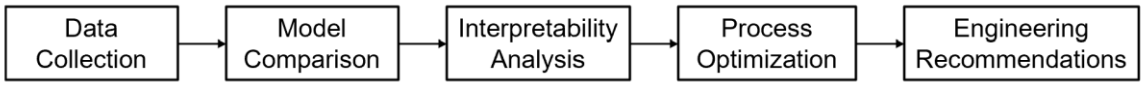


Figure S1. Workflow of the Machine Learning-Based Analysis for Phosphorus Recovery

S.4.Analysis of Anomalous Results

Table S1. Detailed Data Table for Error Analysis (Normalization)

Normalization	MAE	MSE	R2	RMSE	Comprehensive Evaluation
GPR	0.6784	0.4110	0.6901	0.5386	0.6017
RF	0.4164	0.3650	0.6342	0.5093	0.5118
ANN	0.5343	0.3581	0.5100	0.4207	0.4666
XGB	0.6086	0.4126	0.6176	0.5290	0.5571
Elastic Net	0.6240	0.5144	0.4838	0.5606	0.5333
PLSR	0.4309	0.2781	0.4247	0.3381	0.3793

Table S2. Raw error metrics of machine learning models for phosphorus recovery prediction (Part 1/2: GPR, RF , and ANN)

GPR				RF				ANN			
MAE	MSE	R2	RMSE	MAE	MSE	R2	RMSE	MAE	MSE	R2	RMSE
-8.842716143	-157.1640504	0.689551858	-12.5365087	-5.505182014	-86.94127631	0.828263794	-9.324230601	-10.99752755	-222.0404595	0.561400664	-14.90102210
-8.496736803	-100.4119566	0.832769236	-10.02057666	-5.179180569	-56.0047607	0.932372189	-7.483632855	-16.83331573	-384.4423946	0.359731673	-19.60720262
-7.987784299	-431.8330112	0.986256705	-20.78059218	-9.335601953	-151.9234513	0.746979586	-12.32572316	-16.26858477	-749.8106508	0.976136913	-27.38267063
-4.916087291	-200.8053669	0.110715561	-14.17058103	-1.585094340	-23.84364340	0.999241164	-4.882995330	-6.141474406	-85.14282631	0.622937416	-9.227287050
-0.408033084	-1.408170854	0.998791513	-1.186663749	-1.752666667	-14.03464667	0.937846318	-3.746284381	-9.031768322	-174.3463148	0.850376612	-13.20402646
				-0.012500000	-0.002500000	0.999997855	-0.050000000				

Table S2 (continued). Raw error metrics of machine learning models for phosphorus recovery prediction (Part 2/2: XGB, Elastic Net , and PLSR).

XGB				Elastic Net				PLSR			
MAE	MSE	R2	RMSE	MAE	MSE	R2	RMSE	MAE	MSE	R2	RMSE
-4.602836329	-73.10748514	0.855589857	-8.550291524	-12.24173311	-255.3418753	0.495619956	-15.97942037	-11.87057442	-247.4062036	0.511295388	-15.72915140
-4.887059944	-52.04713972	0.937151162	-7.214370362	-16.98571760	-421.9939007	0.297191640	-20.54249013	-14.95097590	-346.8180793	0.422392966	-18.62305236
-8.280540093	-99.93142111	0.833569542	-9.996570467	-17.15867309	-487.8410673	0.984474222	-22.08712447	-24.87604109	-1411.601828	0.955075088	-37.57128994
-1.191024061	-21.88738702	0.999303423	-4.678395774	-4.539091957	-97.63607874	0.567609935	-9.881097042	-4.656781346	-102.3953025	0.546533289	-10.11905641
-0.491414293	-1.676692782	0.992574617	-1.294871724	-11.14385078	-228.9251090	0.803537285	-15.13027128	-10.48990375	-224.0236012	0.807743742	-14.96741799
-0.001654387	-4.667178018	0.999999996	-0.002160365								

S.5.Data Sources for Machine Learning

This study utilized the following data sources for machine learning modeling.

Table S3. Data Sources for Machine Learning

Number	Data Sources for Machine Learning
1	https://doi.org/10.1002/cjce.22799
2	https://link.oversea.cnki.net/doi/10.20025/j.cnki.CN10-1679.2024-22-06
3	https://doi.org/10.1590/S0104-66322008000100003
4	https://link.oversea.cnki.net/doi/10.13438/j.cnki.jdzk.2025.01.008
5	https://doi.org/10.1016/j.jtice.2020.11.031
6	https://doi.org/10.3390/w16111527
7	https://doi.org/10.1007/s12205-014-0070-9
8	https://doi.org/10.1016/j.scitotenv.2021.151109
9	https://doi.org/10.13205/j.hjgc.202205005
10	https://link.oversea.cnki.net/doi/10.16606/j.cnki.issn0253-4320.2007.s1.079
11	https://chn.oversea.cnki.net/KCMS/detail/detail.aspx?dbcode=CJFD&dbname=CJFD-LAST2025&filename=JZJS2024S1077&uniplatform=OVERSEA&v=3OL4dlbeap6w-Ct_SemmKZqWNjHYhRn2_WaoTrlPFTopls_e7NWbQ3jSqU9vyApo
12	https://doi.org/10.1016/j.scitotenv.2021.151109
13	https://doi.org/10.14099/j.cnki.tjkj.2024.06.012
14	https://doi.org/10.1016/j.egypro.2012.05.151
15	https://doi.org/10.16661/j.cnki.1672-3791.2401-5042-0583
16	https://doi.org/10.1007/s12649-019-00724-8
17	https://doi.org/10.1590/S0104-66322008000100003
18	https://doi.org/10.1016/j.chemosphere.2022.136852
19	https://doi.org/10.1002/cjce.22799
20	https://doi.org/10.1016/j.jtice.2020.11.031
21	https://doi.org/10.3390/w16111527
22	https://doi.org/10.1007/s12205-014-0070-9

The specific data for machine learning are presented in Table S4.

Table S4. Dataset for machine learning modeling: Aluminum ion (Al^{3+}) precipitation system (Part 1/3). 12

Input						Output		
Time(min)	Temperature(℃)	Mixing speed(rpm)	pH	inorganic phosphate(mg/L)	Al(mg/L)	Al Phosphorus recovery (%)	Phosphorus recovery equilibrium time(min)	References
12	25	75	8	25.97	110	55.14054678	12	2
12	25	75		25.97	220	89.17982287	12	2
12	25	75		25.97	330	95.87986138	12	2
12	25	75		25.97	440	96.4574509	12	2
12	25	75		25.97	550	97.38159415	12	2
40	25	150	7.07	8.42	10	40	45	4
40	25	150	7.07	8.42	15	51	45	4
40	25	150	7.07	8.42	20	61	45	4
40	25	150	7.07	8.42	30	74	45	4
40	25	150	7.07	8.42	45	86	45	4
40	25	150	7.07	8.42	55	91	45	4
40	25	150	7.07	10.23	15	52	45	4
40	25	150	7.07	10.23	25	75	45	4
40	25	150	7.07	10.23	35	83	45	4
40	25	150	7.07	10.23	40	84	45	4
40	25	150	7.07	10.23	50	88	45	4
40	25	150	7.07	10.23	55	86	45	4

40	25	150	7.0 7	13.93	10	60	45	4
40	25	150	7.0 7	13.93	20	75	45	4
40	25	150	7.0 7	13.93	30	84	45	4
40	25	150	7.0 7	13.93	45	88	45	4
40	25	150	7.0 7	13.93	55	92	45	4
40	25	150	7.0 7	13.93	60	94	45	4
20	20		8	10	5	80	80	6
40	20		8	10	5	81	80	6
60	20		8	10	5	82	80	6
80	20		8	10	5	81	80	6
20	20		9	10	5	52	80	6
40	20		9	10	5	57	80	6
60	20		9	10	5	60	80	6
80	20		9	10	5	58.5	80	6
20	20		10	10	5	92	80	6
40	20		10	10	5	82	80	6
60	20		10	10	5	81	80	6
80	20		10	10	5	81.5	80	6
30	20		8	5.6	2.5	76.78571429	30	11
30	20		8	5.6	5	83.03571429	30	11
30	20		8	5.6	7.5	87.5	30	11
30	20		8	5.6	10	90.17857143	30	11
30	20		8	5.6	12.5	92.85714286	30	11
30	20		8	5.6	15	94.64285714	30	11
30	20		8	5.6	17.5	95.89285714	30	11
30	20		8	5.6	20	95.17857143	30	11
30	20		8	5.6	22.5	95.71428571	30	11

30	20		8	5.6	25	96.25	30	11
30	20		8	5.6	3.15	66.07142857	30	11
30	20		8	5.6	6.31	75.53571429	30	11
30	20		8	5.6	9.46	85.35714286	30	11
30	20		8	5.6	12.62	87.5	30	11
30	20		8	5.6	15.77	89.28571429	30	11
30	20		8	5.6	18.92	89.82142857	30	11
30	20		8	5.6	22.08	90.17857143	30	11
30	20		8	5.6	25.23	91.96428571	30	11
30	20		8	5.6	28.39	95	30	11
30	20		8	5.6	31.54	95.71428571	30	11
5	20			10	11.7	49		13
10	20			10	11.7	48		13
15	20			10	11.7	48.5		13
20	20			10	11.7	47.5		13
25	20			10	11.7	48		13
30	20			10	11.7	47.7		13
43	25	100	6.5	0.94	0.2	89	50	14
43	25	100	6.5	0.94	0.4	82	50	14
43	25	100	6.5	0.94	0.6	77	50	14
43	25	100	6.5	0.94	0.8	70	50	14
43	25	100	6.5	0.94	1	68	50	14
43	25	100	6.5	0.94	1.2	63	50	14
43	25	100	6.5	0.94	1.4	60	50	14
43	25	100	6.5	0.94	1.6	57	50	14
43	25	100	6.5	0.94	1.8	55	50	14
43	25	100	6.5	0.94	2	50	50	14
43	25	100	7	0.94	0.2	90	50	14
43	25	100	7	0.94	0.4	81	50	14
43	25	100	7	0.94	0.6	80	50	14
43	25	100	7	0.94	0.8	70	50	14
43	25	100	7	0.94	1	68	50	14
43	25	100	7	0.94	1.2	64	50	14

43	25	100	7	0.94	1.4	62	50	14
43	25	100	7	0.94	1.6	57	50	14
43	25	100	7	0.94	1.8	52	50	14
43	25	100	7	0.94	2	50	50	14
43	25	100	7.5	0.94	0.2	90	50	14
43	25	100	7.5	0.94	0.4	84	50	14
43	25	100	7.5	0.94	0.6	79	50	14
43	25	100	7.5	0.94	0.8	71	50	14
43	25	100	7.5	0.94	1	68	50	14
43	25	100	7.5	0.94	1.2	65	50	14
43	25	100	7.5	0.94	1.4	60	50	14
43	25	100	7.5	0.94	1.6	57	50	14
43	25	100	7.5	0.94	1.8	53	50	14
43	25	100	7.5	0.94	2	50	50	14
43	25	100	8	0.94	0.2	90	50	14
43	25	100	8	0.94	0.4	82	50	14
43	25	100	8	0.94	0.6	78	50	14
43	25	100	8	0.94	0.8	72	50	14
43	25	100	8	0.94	1	70	50	14
43	25	100	8	0.94	1.2	68	50	14
43	25	100	8	0.94	1.4	63	50	14
43	25	100	8	0.94	1.6	60	50	14
43	25	100	8	0.94	1.8	57	50	14
43	25	100	8	0.94	2	52	50	14
32	20	60		1.1	5.71	83.63636364	40	15
32	20	60		1.1	7.14	88.18181818	40	15
32	20	60		1.1	8.57	90	40	15
32	20	60		1.1	12.38	90	40	15
60	20	150	5	750	1180	95	60	19
60	20	150	6	750	1180	99	60	19
60	20	150	7	750	1180	98	60	19
60	20	150	8	750	1180	97.01333333	60	19
60	20	150	9	750	1180	88	60	19

60	20	150	10	750	1180	82	60	19
41	20	50	4	6.5	10.2	77	50	20
41	20	50	5	6.5	10.2	80	50	20
41	20	50	6	6.5	10.2	82.5	50	20
41	20	50	7	6.5	10.2	78.5	50	20
41	20	50	8	6.5	10.2	72.5	50	20
41	20	50	9	6.5	10.2	71	50	20
41	20	50	4	1.7	2.66	76.47352941	50	20
41	20	50	5	1.7	2.66	80	50	20
41	20	50	6	1.7	2.66	81.5	50	20
41	20	50	7	1.7	2.66	79	50	20
41	20	50	8	1.7	2.66	72	50	20
41	20	50	9	1.7	2.66	70.5	50	20
41	20	50	4	18	28.2	72.5	50	20
41	20	50	5	18	28.2	78.5	50	20
41	20	50	6	18	28.2	82.5	50	20
41	20	50	7	18	28.2	75	50	20
41	20	50	8	18	28.2	72.5	50	20
41	20	50	9	18	28.2	70	50	20
41	20	50	4	96	150	72	50	20
41	20	50	5	96	150	78	50	20
41	20	50	6	96	150	75	50	20
41	20	50	7	96	150	72	50	20
41	20	50	8	96	150	68	50	20
41	20	50	9	96	150	66	50	20
41	20	50	4	30	47	217.6	50	20
41	20	50	5	30	47	230.4	50	20
41	20	50	6	30	47	225.6	50	20
41	20	50	7	30	47	217.6	50	20
41	20	50	8	30	47	212.8	50	20
41	20	50	9	30	47	208.16	50	20
50	25	100	6.4	17.83	45	50	50	21
50	25	100	6.7	17.83	45	90	50	21

50	25	100	7	17.83	45	92	50	21
50	25	100	7.2	17.83	45	88	50	21
50	25	100	7.5	17.83	45	87	50	21
50	25	100	7.7	17.83	45	97	50	21

13

Table S4(continued). Dataset for machine learning modeling: Aluminum ion (Ca^{2+}) precipitation system (Part 2/3). 14

Input						Output		
Time(min)	Temperature(℃)	Mixing speed(rpm)	pH	Inorganic phosphate(mg/L)	Ca（mg/L）	Ca_ Phosphorus recovery (%)	Phosphorus recovery equilibrium time(min)	References
30	25	100	9	20300	13975	68.49753695	30	1
60	22	60	11	2	1.25	90.5	120	5
60	22	60	9.5	2	2	94	120	5
60	22	60	9.5	2	1.25	74.8	120	5
60	22	60	9.5	2	1.25	93.8	120	5
60	22	60	11	2	1.25	76.3	120	5
60	22	60	9.5	2	0.5	72.3	120	5
60	22	60	8	2	1.25	78.3	120	5
60	22	60	8	2	1.25	72.3	120	5
60	22	60	8	2	2	69.1	120	5
60	22	60	11	2	1.25	94.2	120	5
60	22	60	9.5	2	1.25	96	120	5
60	22	60	11	2	1.25	95.6	120	5
60	22	60	9.5	2	1.25	96.5	120	5
60	22	60	9.5	2	0.5	98.6	120	5
60	22	60	11	2	0.5	97.3	120	5
60	22	60	9.5	2	0.5	97.6	120	5
60	22	60	9.5	2	0.5	97.7	120	5
10	20	150	8	10	50	19	30	6
20	20	150	8	10	50	12	30	6
30	20	150	8	10	50	20	30	6
10	20	150	9	10	50	67	30	6
20	20	150	9	10	50	78	30	6
30	20	150	9	10	50	70	30	6

10	20	150	10	10	50	81	30	6
20	20	150	10	10	50	80	30	6
30	20	150	10	10	50	78	30	6
50	20	250	7	100	200	48	50	10
50	20	250	8	100	200	55	50	10
50	20	250	9	100	200	62	50	10
50	20	250	10	100	200	60	50	10
50	20	250	11	100	200	53	50	10
50	20	250	12	100	200	58	50	10
50	20	250	10	105.8	100	26.89981096	50	10
50	20	250	10	105.8	200	47.65595463	50	10
50	20	250	10	105.8	300	61.97542533	50	10
50	20	250	10	105.8	400	73.96030246	50	10
50	20	250	10	105.8	500	90.62381853	50	10
50	20	250	10	91.26	100	38.13280736	50	10
50	20	250	10	91.26	200	54.74468551	50	10
50	20	250	10	91.26	300	70.33749726	50	10
50	20	250	10	91.26	400	85.8974359	50	10
50	20	250	10	91.26	500	92.40631164	50	10
5	20	160	7	470	742	15.78723404	40	16
10	20	160	7	470	742	29.99574468	40	16
15	20	160	7	470	742	44.20425532	40	16
20	20	160	7	470	742	56.83404255	40	16
25	20	160	7	470	742	61.57021277	40	16
30	20	160	7	470	742	67.88510638	40	16
35	20	160	7	470	742	78.93617021	40	16
40	20	160	7	470	742	89.98723404	40	16
5	20	160	7	470	695.4	29	40	16
10	20	160	7	470	695.4	38	40	16
15	20	160	7	470	695.4	42	40	16
20	20	160	7	470	695.4	49	40	16
25	20	160	7	470	695.4	57	40	16
30	20	160	7	470	695.4	61	40	16

35	20	160	7	470	695.4	67	40	16
40	20	160	7	470	695.4	72	40	16
5	40	160	7	470	695.4	32	40	16
10	40	160	7	470	695.4	36	40	16
15	40	160	7	470	695.4	44	40	16
20	40	160	7	470	695.4	53	40	16
25	40	160	7	470	695.4	66	40	16
30	40	160	7	470	695.4	70	40	16
35	40	160	7	470	695.4	78	40	16
40	40	160	7	470	695.4	82	40	16
5	40	160	7	470	742	12	40	16
10	40	160	7	470	742	26	40	16
15	40	160	7	470	742	33	40	16
20	40	160	7	470	742	38	40	16
25	40	160	7	470	742	45	40	16
30	40	160	7	470	742	49	40	16
35	40	160	7	470	742	55	40	16
40	40	160	7	470	742	60	40	16
60	20	150	5	750	1550	5	60	19
60	20	150	6	750	1550	32	60	19
60	20	150	7	750	1550	77	60	19
60	20	150	8	750	1550	86	60	19
60	20	150	9	750	1550	96	60	19
60	20	150	10	750	1550	99	60	19

Table S4 (continued). Dataset for machine learning modeling: Aluminum ion (Fe^{3+}) precipitation system (Part 3/3)

Input						Output		
Time(min)	Temperature(℃)	Mixing speed(rpm)	pH	inorganic phosphate(mg/L)	Fe(mg/L)	Fe Phosphorus recovery (%)	Phosphorus recovery equilibrium time(min)	References
	25		4.5	3.9	5.07	77.94871795		3
40	25	150	7.07	8.42	10	40	45	4
40	25	150	7.07	8.42	15	51	45	4
40	25	150	7.07	8.42	20	61	45	4

40	25	150	7.07	8.42	30	74	45	4
40	25	150	7.07	8.42	45	86	45	4
40	25	150	7.07	8.42	55	91	45	4
40	25	150	7.07	10.23	15	52	45	4
40	25	150	7.07	10.23	25	75	45	4
40	25	150	7.07	10.23	35	83	45	4
40	25	150	7.07	10.23	40	84	45	4
40	25	150	7.07	10.23	50	88	45	4
40	25	150	7.07	10.23	55	86	45	4
40	25	150	7.07	13.93	10	60	45	4
40	25	150	7.07	13.93	20	75	45	4
40	25	150	7.07	13.93	30	84	45	4
40	25	150	7.07	13.93	45	88	45	4
40	25	150	7.07	13.93	55	92	45	4
40	25	150	7.07	13.93	60	94	45	4
720	20	60	6.7	1600	1600	56.25	720	5
720	20	60	6.9	1600	1600	10.625	720	5
720	20	60	7.1	1600	1600	15.625	720	5
720	20	60	7.3	1600	1600	25.625	720	5
720	20	60	6.8	1600	3200	37.5	720	5
720	20	60	7	1600	3200	7.1875	720	5
720	20	60	7.2	1600	3200	10	720	5
720	20	60	7.4	1600	3200	23.75	720	5
720	20	60	6.7	1600	2400	3.125	720	5
720	20	60	6.8	1600	2400	4.0625	720	5
720	20	60	6.9	1600	2400	6.5625	720	5
720	20	60	7.1	1600	2400	10	720	5
720	20	60	7.3	1600	2400	15.625	720	5
20	20		6	10	7.5	89	80	6
40	20		6	10	7.5	90	80	6
60	20		6	10	7.5	92	80	6
80	20		6	10	7.5	95	80	6
20	20		7	10	7.5	82	80	6

40	20		7	10	7.5	81	80	6
60	20		7	10	7.5	83	80	6
80	20		7	10	7.5	84	80	6
50	20	50	4	1.17	2	50	50	7
50	20	50	5	1.17	2	57	50	7
50	20	50	6	1.17	2	61	50	7
50	20	50	6.5	1.17	2	58	50	7
50	20	50	7	1.17	2	64	50	7
50	20	50	8	1.17	2	52	50	7
50	20	50	9	1.17	2	37	50	7
50	20	50	4	1.17	4	59	50	7
50	20	50	5	1.17	4	64	50	7
50	20	50	6	1.17	4	70	50	7
50	20	50	6.5	1.17	4	73.5042735	50	7
50	20	50	7	1.17	4	71	50	7
50	20	50	8	1.17	4	66	50	7
50	20	50	9	1.17	4	56	50	7
50	20	50	4	1.17	6	62	50	7
50	20	50	5	1.17	6	69	50	7
50	20	50	6	1.17	6	80	50	7
50	20	50	6.5	1.17	6	76	50	7
50	20	50	7	1.17	6	74	50	7
50	20	50	8	1.17	6	72	50	7
50	20	50	9	1.17	6	63	50	7
50	20	50	4	1.17	8	70	50	7
50	20	50	5	1.17	8	75	50	7
50	20	50	6	1.17	8	94	50	7
50	20	50	6.5	1.17	8	92	50	7
50	20	50	7	1.17	8	90	50	7
50	20	50	8	1.17	8	86	50	7
50	20	50	9	1.17	8	72	50	7
50	20	50	4	1.17	12	80	50	7
50	20	50	5	1.17	12	88	50	7

50	20	50	6	1.17	12	97.5042735	50	7
50	20	50	6.5	1.17	12	100	50	7
50	20	50	7	1.17	12	96	50	7
50	20	50	8	1.17	12	91	50	7
50	20	50	9	1.17	12	81	50	7
50	20			10.5	24.62	99.5	50	7
50	20			4.6	16.6	84.7	50	8
50	20			2.9	12.56	91	50	8
50	20			4.2	3.79	84.7	50	8
50	20			8.7	3.14	85	50	8
50	20			14.5	2.61	90	50	8
50	20			6.35	20.61	95.6	50	8
50	20			4.97	20.61	85.4	50	8
50	20			9.18	62.09	94.17211329	50	8
40	20	150	7	410	797.5	98	40	9
40	20	150	11.45	410	797.5	97	40	9
40	20	150	11.75	410	797.5	98	40	9
40	20	150	11.93	410	797.5	98.5	40	9
40	20	150	12.05	410	797.5	99	40	9
40	20	150	12.15	410	797.5	99.5	40	9
40	20	150	12.23	410	797.5	96	40	9
40	20	150	12.3	410	797.5	97.5	40	9
40	20	150	12.36	410	797.5	96.5	40	9
40	20	150	12.4	410	797.5	92	40	9
30	20		8	5.6	6.88	67.85714286	30	11
30	20		8	5.6	13.76	86.60714286	30	11
30	20		8	5.6	20.64	92.5	30	11
30	20		8	5.6	27.52	94.64285714	30	11
30	20		8	5.6	34.4	96.07142857	30	11
30	20		8	5.6	41.28	96.33928571	30	11
30	20		8	5.6	48.16	96.42857143	30	11
30	20		8	5.6	55.04	96.33928571	30	11
30	20		8	5.6	61.92	96.42857143	30	11

30	20	8	5.6	68.8	96.32142857	30	11
30	20	8	5.6	4.02	71.07142857	30	11
30	20	8	5.6	8.04	83.92857143	30	11
30	20	8	5.6	12.05	87.5	30	11
30	20	8	5.6	16.07	91.07142857	30	11
30	20	8	5.6	20.09	92.5	30	11
30	20	8	5.6	24.11	93.21428571	30	11
30	20	8	5.6	28.13	93.57142857	30	11
30	20	8	5.6	32.14	93.92857143	30	11
30	20	8	5.6	36.16	94.64285714	30	11
30	20	8	5.6	40.18	95	30	11
30	20	7	60	79.75	48.22	60	12
30	20	7	60	79.75	45.76	60	12
30	20	7	60	159.5	79.07	60	12
30	20	7	60	159.5	79.5	60	12
30	20	7	60	239.25	93.69	60	12
30	20	7	60	239.25	97.17	60	12
30	20	7	60	159.5	80.21	60	12
30	20	7	60	159.5	80.06	60	12
30	20	7	60	159.5	79.65	60	12
30	20	6.5	60	79.75	50.22	60	12
30	20	6.5	60	159.5	81.31	60	12
30	20	6.5	60	239.25	97.85	60	12
30	20	6.5	60	159.5	79.52	60	12
30	20	7.5	60	159.5	73.56	60	12
30	20	7.5	60	159.5	78.02	60	12
30	20	7.5	60	79.75	41.75	60	12
30	20	7.5	60	239.25	96.25	60	12
5	20		10	12	62		13
10	20		10	12	64		13
15	20		10	12	65		13
20	20		10	12	66		13
25	20		10	12	66		13

30	20			10	12	65		13
32	20	60		1.1	0.96	81.81818182	40	15
32	20	60		1.1	1.2	89.09090909	40	15
32	20	60		1.1	1.4	90.90909091	40	15
32	20	60		1.1	2.08	93.63636364	40	15
40	25	40	3	80	150	55	40	17
40	25	40	5	80	150	65	40	17
40	25	40	6	80	150	69	40	17
40	25	40	7	80	150	74	40	17
40	25	40	8	80	150	83	40	17
40	25	40	10	80	150	88	40	17
40	25	40	11	80	150	95.5	40	17
40	25	40	12	80	150	99	40	17
40	25	40	3.5	80	100	33	40	17
40	25	40	4	80	100	34.5	40	17
40	25	40	5	80	100	41	40	17
40	25	40	7	80	100	52	40	17
40	25	40	8	80	100	67.125	40	17
40	25	40	9	80	100	77	40	17
40	25	40	10	80	100	90	40	17
40	25	40	11	80	100	96	40	17
40	25	40	5.5	80	50	24	40	17
40	25	40	6	80	50	29	40	17
40	25	40	7	80	50	39	40	17
40	25	40	7.5	80	50	46	40	17
40	25	40	8	80	50	57	40	17
40	25	40	9	80	50	68	40	17
40	25	40	10	80	50	82	40	17
40	25	40	10.5	80	50	91.125	40	17
40	25	40	11	80	50	96	40	17
40	25	40	12	80	50	97	40	17
10	20	80	4.3	10	36.08	74	100	18
20	20	80	4.3	10	36.08	76	100	18

30	20	80	4.3	10	36.08	77.5	100	18
60	20	80	4.3	10	36.08	79	100	18
80	20	80	4.3	10	36.08	80	100	18
100	20	80	4.3	10	36.08	81.5	100	18
10	20	80	5.3	10	36.08	98	100	18
20	20	80	5.3	10	36.08	98	100	18
30	20	80	5.3	10	36.08	98	100	18
60	20	80	5.3	10	36.08	97	100	18
80	20	80	5.3	10	36.08	97	100	18
100	20	80	5.3	10	36.08	96	100	18
10	20	80	6.3	10	36.08	95	100	18
20	20	80	6.3	10	36.08	96.5	100	18
30	20	80	6.3	10	36.08	97	100	18
60	20	80	6.3	10	36.08	98	100	18
80	20	80	6.3	10	36.08	97	100	18
100	20	80	6.3	10	36.08	96	100	18
10	20	80	7.3	10	36.08	95	100	18
20	20	80	7.3	10	36.08	96.5	100	18
30	20	80	7.3	10	36.08	97	100	18
60	20	80	7.3	10	36.08	98	100	18
80	20	80	7.3	10	36.08	98	100	18
100	20	80	7.3	10	36.08	98	100	18
10	20	80	4.7	10	18	87	100	18
20	20	80	4.7	10	18	86	100	18
30	20	80	4.7	10	18	86.7	100	18
60	20	80	4.7	10	18	89.8	100	18
80	20	80	4.7	10	18	88.5	100	18
100	20	80	4.7	10	18	88	100	18
10	20	80	4.7	10	36.1	96	100	18
20	20	80	4.7	10	36.1	97	100	18
30	20	80	4.7	10	36.1	98	100	18
60	20	80	4.7	10	36.1	99	100	18
80	20	80	4.7	10	36.1	98.6	100	18

100	20	80	4.7	10	36.1	98	100	18
10	20	80	4.7	10	54.1	99	100	18
20	20	80	4.7	10	54.1	99	100	18
30	20	80	4.7	10	54.1	99	100	18
60	20	80	4.7	10	54.1	99.5	100	18
80	20	80	4.7	10	54.1	99	100	18
100	20	80	4.7	10	54.1	99	100	18
60	20	150	5	750	2430	99	60	19
60	20	150	6	750	2430	97	60	19
60	20	150	7	750	2430	93	60	19
60	20	150	8	750	2430	91.5	60	19
60	20	150	9	750	2430	82	60	19
60	20	150	10	750	2430	74	60	19
41	20	50	4	6.5	21.1	85	50	20
41	20	50	5	6.5	21.1	88	50	20
41	20	50	6	6.5	21.1	82.5	50	20
41	20	50	7	6.5	21.1	79.5	50	20
41	20	50	8	6.5	21.1	71	50	20
41	20	50	9	6.5	21.1	65	50	20
41	20	50	4	1.7	5.52	81	50	20
41	20	50	5	1.7	5.52	87.5	50	20
41	20	50	6	1.7	5.52	82.48823529	50	20
41	20	50	7	1.7	5.52	76.5	50	20
41	20	50	8	1.7	5.52	64.5	50	20
41	20	50	9	1.7	5.52	62.5	50	20
41	20	50	4	18	58.4	81.5	50	20
41	20	50	5	18	58.4	79	50	20
41	20	50	6	18	58.4	74	50	20
41	20	50	7	18	58.4	68	50	20
41	20	50	8	18	58.4	64	50	20
41	20	50	9	18	58.4	60	50	20
41	20	50	4	96	311	75.5	50	20
41	20	50	5	96	311	72.5	50	20

41	20	50	6	96	311	68	50	20
41	20	50	7	96	311	62	50	20
41	20	50	8	96	311	58	50	20
41	20	50	9	96	311	56	50	20
41	20	50	4	30	97.4	71.5	50	20
41	20	50	5	30	97.4	70.5	50	20
41	20	50	6	30	97.4	64	50	20
41	20	50	7	30	97.4	61.5	50	20
41	20	50	8	30	97.4	57	50	20
41	20	50	9	30	97.4	55	50	20
50	25	100	6.4	17.83	18	50	50	21
50	25	100	6.7	17.83	18	90	50	21
50	25	100	7	17.83	18	92	50	21
50	25	100	7.2	17.83	18	88	50	21
50	25	100	7.5	17.83	18	87	50	21
50	25	100	7.7	17.83	18	97	50	21
40	20	100	8.9	158.2	41.3	20.06321113	40	22
40	20	100	8.9	158.2	82.6	57.18015171	40	22
40	20	100	8.9	158.2	123.9	66.20859671	40	22
40	20	100	8.9	158.2	165.2	78.2300885	40	22
40	20	100	8.9	158.2	206.5	82.25916561	40	22
40	20	100	8.9	158.2	247.8	89.28128951	40	22
40	20	100	8.9	158.2	289.1	92.29077118	40	22
40	20	100	6	158.2	290	76.24020228	40	22
40	20	100	7	158.2	290	95.30025284	40	22
40	20	100	8	158.2	290	91.7891909	40	22
40	20	100	9	158.2	290	88.27812895	40	22
40	20	100	10	158.2	290	70.72281922	40	22